JOURNAL OF MECHANICS OF CONTINUA AND MATHEMATICAL SCIENCES
www.journalimcms.org

ISSN (Online) : 2454 -7190 Vol.-19, No.-6, June (2024) pp 67-79 ISSN (Print) 0973-8975

A COMPREHENSIVE DESIGN AND SIMULATION OF QUADRUPOLE ELECTROMAGNETIC LINEAR SYSTEMS FOR PRECISE POSITIONING IN AEROSPACE

Kintali Manohar[1], Kondamudi Srichandan[2]

[1, 2] Department of EECE, GITAM School of Technology, GITAM deemed to be University, Visakhapatnam, India.

Email: [1]mkintali@gitam.edu , [2]skondamu@gitam.edu

Corresponding Author: **Kintali Manohar**

Email: mkintali@gitam.edu

https://doi.org/10.26782/jmcms.2024.06.00006

(Received: March 22, 2024; Revised: May 18, 2024; Accepted: June 04, 2024)

Abstract

For linear motion applications, particularly in aerospace, this study outlines the creation of an essential Quadrupole Electromagnetic System (QES) as a substitute for a four-track electromagnetic launcher. The QES design is compared with a four-track system to address concerns regarding rail-armature contact sliding. In a QES, four coils provide a homogeneous electromagnetic field, resulting in a Lorentz force on the slider. The QES was designed using the three-dimensional modeling capabilities of the ANSYS software. The results of the magnetic properties show a high potential for scaling this model to various levels. Additionally, the QES power circuit was simulated using ANSYS Simplorer. The circuit uses silicon-controlled rectifiers (SCR) and a pulse-width modulation (PWM) pulse generator. A force of 4kN was achieved, and this paper presents the current and force plots in detail. The study includes finite element analysis, electromagnetic and current characteristics simulation, and monitoring of the skin and proximity effects. Performance is increased by optimizing the QES design parameters using Particle Swarm Optimization (PSO). The simulation results demonstrate the feasibility and scalability of the QES design.

Keywords*:* Electromagnetics, Finite element analysis, Four-track electromagnetic launcher, Particle Swarm Optimization (PSO)

I. Introduction

The automation industry has experienced considerable growth in using positional linear motion drives for robotic activities, including conveyors, sliders, and workbench tasks. This trend is driven by the industry's need for more control and accuracy, resulting in significant opportunities for research and development. Linear drivers rely on two fundamental concepts. First, they transform rotational motion into linear motion, allowing the system to precisely translate the spinning motion of the motor along a single axis. This feature enables the precise movement of items or

components along a straight route. Second, specific linear drives create linear motion without needing extra components, thereby decreasing the possible causes of inaccuracy or inefficiency. Linear electric motors have several advantages for linear motion drives. They minimize friction compared to other technologies, resulting in smoother and more accurate motion and improved control and precision in robotic operations. Linear drive systems are also easier to configure and use than alternative motion control systems, saving time and effort during deployment and maintenance. Furthermore, linear electric motors have an extensive speed range, allowing for various applications in the automation industry, running at varied speeds depending on the needs and optimizing the performance.

Numerous studies [XII], [XIII], [XIV], [XV], [XVIII]. have described the advantages of linear electric motors for enhanced control and precision in various fields. Recent research has focused on developing linear motors for robotic applications, such as creating and optimizing motors for high-speed robotic applications, self-sensing capabilities, modular designs, and high-performance characteristics. These developments have helped increase the control and precision of robotic applications.

Proposed a multipole electromagnetic device with force and velocity characteristics. [XXI] Building on this work, [XXIV] Investigated a Multipole Field Electromagnetic Launcher (MFEL) model featuring a double-sided armature and enhanced flux density by positioning the coil both inside and outside the armature in a coaxial manner. To counterbalance the magnetic attraction caused by rotational motion. [IX], [XV], [XVI], [XXVI] presented the notion of multistage twisted multipole electromagnetic launching, in which an armature accelerates and spins around its axis. Additionally, the authors suggested an evacuated-tube launch mechanism based on the intriguing idea of multipole field launching for vehicle applications. Several investigations have been undertaken to investigate further the possibilities of MFEL, including flux distribution studies and studies into different armature forms and ideal designs.

Inspired by a Multipole Electromagnetic Launcher, this study introduces a Quadrupole Electromagnetic System (QES). A 3D model of the QES was created, and the flow characteristics were analyzed using ANSYS to examine the variances in different areas of the model. The proposed QES model is promising for using square-shaped rod supports in various motion-tracking systems.

This study examines a Quadrupole Electromagnetic System (QES) algorithm design and model for linear movement tracking in manufacturing industries. QES is a highly accurate non-contact sensor for measuring the velocity and position of objects in motion. It provides thorough details of the algorithm design, including magnetic material selection, magnetic field strength calculation, and accurate sensor positioning. In addition, the paper discusses the QES algorithm and its model, which were based on finite element analysis (FEA); the magnetic field was simulated using finite element analysis, and ANSYS was used to analyze the data. This explains the theoretical foundations of QES, including the magnetic field principles and quadrupole design. Integrating QES in industrial manufacturing systems offers advantages such as precise positioning with control over objects and effective detection of diversions from the actual path, resulting in improved product standards and waste reduction. In conclusion, the article's comprehensive coverage of the algorithm design and model of QES systems

with linear motion tracking applications provides valuable insights into advancing and implementing this technology in various manufacturing sectors. All the coils must be excited simultaneously with the same current magnitude to produce a uniform magnetic field on the object. When this magnetic field interacts with the primary magnetic field by inducing eddy currents within the object, the system's Lorentz force is generated.

II. Design structure of QES

With four coils mounted on a square yoke, quadrupole electromagnetic systems were constructed based on the electromagnetic induction principle. The primary objective of this design is to apply it to a motion track system, specifically to a robotic arm positioning system.

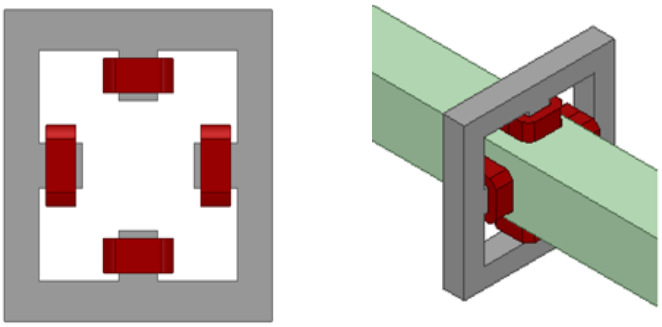

Fig. 1. 3D model of the QES

Fig. 1 shows a 3D model developed using ANSYS, with an analysis considering 1000 turns for the coils. Using copper as the coil material, the coil's dimensions were 40 mm in the x, 40 mm in the y, and 68 mm in the z direction. Iron was used to construct the yoke, which has dimensions of 153 mm in the x, 22 mm in the y, and 20 mm in the z directions.

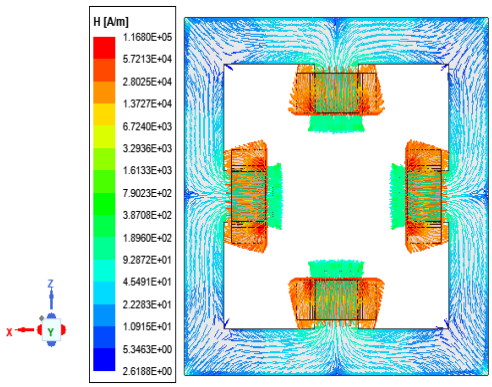

Fig 2. QES Yoke and Coil Magnetic Intensity Vectors

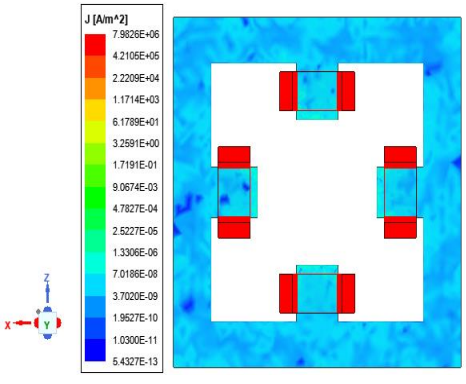

Fig 3. Current density in the yoke and coils of QES

The model considers the following iron parameters: a bulk conductivity of 103 × 105 siemens/m, a relative conductivity of 4000, and a Poisson's ratio of 0.28. It has been proposed that the center bar be made of iron for simplicity in analysis and ease of examination. The iron used in this experiment has the following properties: relative conductivity of 4000, Poisson's ratio of 0.28, and conductivity of 103 × 105 siemens/m. We investigated the magnetic characteristics of the QES by magnetostatic analysis using ANSYS Maxwell and a current excitation of 1000 A. The magnetic flux density patterns of the QES concerning vectors and magnitude are shown in Fig. 2.

The coils exhibit the maximum magnetic field intensity of the magnetic system, reaching a maximum of 1.168 × 105 A/m and a minimum of 2.61 A/m. The field was uniform within the yoke, and the magnetic density was 3.58 Tesla. The electric current flowing through the coil determines the intensity of the magnetic field, and the current strength affects the direction and size of the field. Fig. 3 depicts a plot of the current density, with the yoke being somewhat colder than the coils and the maximum current density in the coils, signifying the hottest areas.

III. QES for linear motion tracking

Modern robotics faces a continuous increase in complexity and expenses, which demands flexible automation, such as linear motion system tracks, for increased workspace. However, these tracks reduce the accuracy compared to the precise use of robotic systems in industrial applications [24]. Identifying nonlinearities in a linear path is necessary to enhance the precision of robotic linear-track systems.

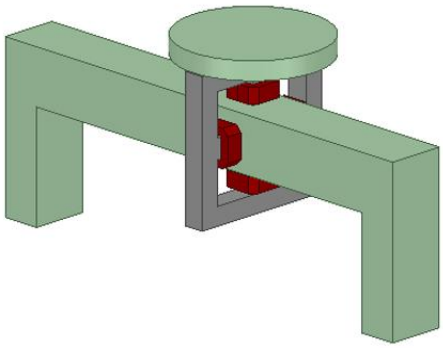

Fig. 4. 3D model of Linear motion tracking system with QES

Integrated track motions and linear motion tracking in industrial production applications greatly influence the design of QES systems. A three-dimensional schematic of the QES-based linear motion track, integrating track movements, is depicted in Fig.4, which includes a model that features a non-conducting plate mounted over the yoke, with a low-electrical-resistance plate serving as the utility place. The industrial operation area determines the variation in sliding bar length. In Fig. 4, a 1000A current was injected into the coils for testing. The results of the 3D FEM show that the coils in the yoke pole

shoes, as shown in Fig. 5, have a maximum peak intensity, current density, and flux density of 3.5839 Tesla.

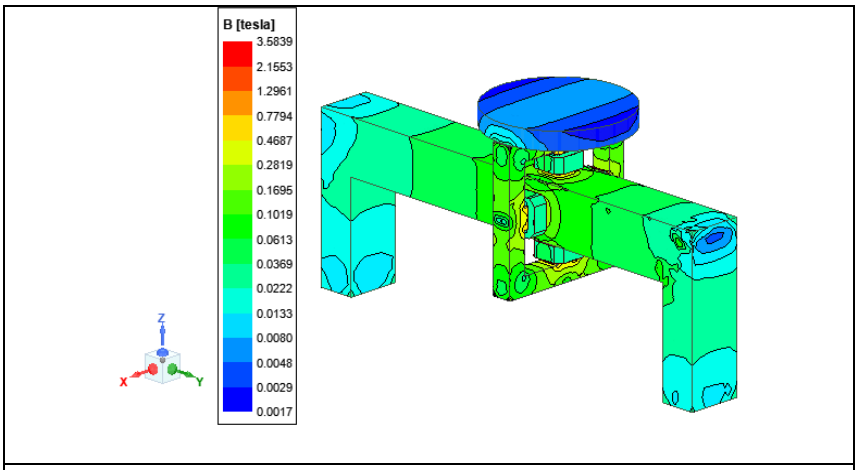

Fig. 5. Magnetic density in Linear motion tracking system with QES

The Fig. 5 indicates relatively stronger magnetic field strength near the electromagnet poles and weaker in the center.

IV. Design Optimization

For the optimal design of the QES, obtaining the objective function is essential. Obtaining the maximum velocity with minimum power consumption is the main motto of this section. The objective of the design of QES is to get the best force considering the design constraints.

$$F_{best} = f(l_c, h_c, l_g, l_b, w_b, N, nol) \tag{1}$$

subjected to

Coil thickness as a constraint.

$$0 < t < t_{max} \tag{2}$$

Coil length as a constraint.

$$0 < l_c < l_{max} \tag{3}$$

Where nop is abbreviated as the number of poles, l_c is the length of the coil, h_c is coil height, l_g is air-gap length, l_b is the bar length, w_b is the bar width, and N is the total number of rotations.
The formulae on which PSO works are given as

$$v_i^{k+1} = w_i v_i^k + c_1 rand(P_{besti} - S_i^k) + c_2 rand(g_{best} - S_i^k) \tag{4}$$

where

$v_i^k = current\ velocity\ of\ agent\ i\ at\ iteration\ k$

$w = w_{max} - \frac{w_{max} - w_{min}}{iter_{max}} * iter$

$rand = the\ random\ number\ between\ 0\ and\ 1$

$S_i^k = current\ position\ of\ agent\ i\ at\ iteration\ k$

$c_i = weight\ coefficient\ for\ each\ term$

$P_{besti} = Pbest\ of\ agent, i$

$g_{best} = g_{best} of\ the\ group$

$w_i = weight\ function\ for\ velocity\ of\ agent\ i$

Table 1 lists the design input requirements that were considered for the design.

Table 1 : Input Parameters

Parameters	Values
Air permeability	4Π*10^-7 H/m
Pure iron permeability	5000
Wire diameter	0.33 mm
Air-gap length	1 mm
Bar side length	20 mm
Population size	100
Maximum iteration	100
Maximum length of coil	20 mm
Maximum thickness of the coil	10 m

Table 2 : Optimized values

Parameters	Obtained Values
Force Obtained	132 N
Turns number per layer	22
Number of turns	600.36 ~ 601
Coil height	8.712 mm
Coil thickness	5.925 mm
Best value is achieved at run	9th
Population number	8

The optimal design parameters are tabulated after applying the PSO to the design problem, as shown in Table 2. The PSO algorithm is executed ten times, and the best values are tabulated. It is noticed that the highest and lowest equivalent inductances are 0.0164 mH and 0.0172 mH, respectively.

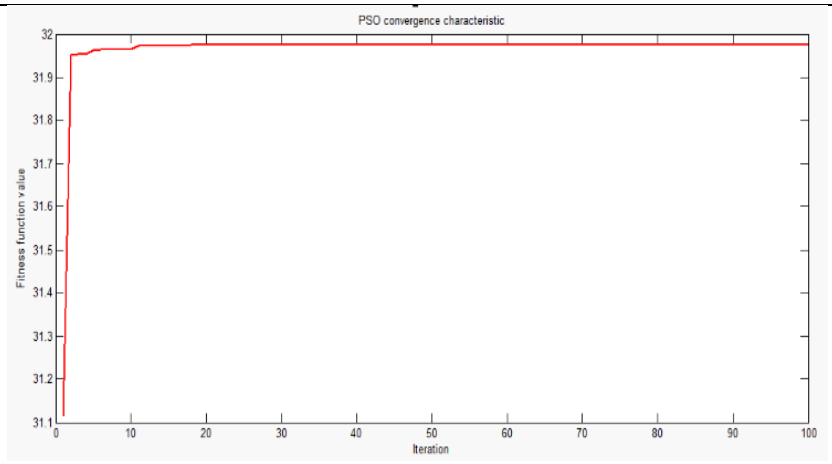

Fig. 6. PSO convergence characteristics

V. Results and Discussions

ANSYS Simplorer simulates the electric side of the QES power circuit. The location and the current are the input variables, while the output variable is the Lorentz force, which is determined by an initial input voltage of 30V. The circuit has resistance R4 (0.001 Ω) and R6 (0.2 Ω). During testing, the PWM switch was used as a switching device with a 0.5-duty cycle and a 20 msec duration. The initial value is set to 0.5 duty cycle and 1 msec delay.

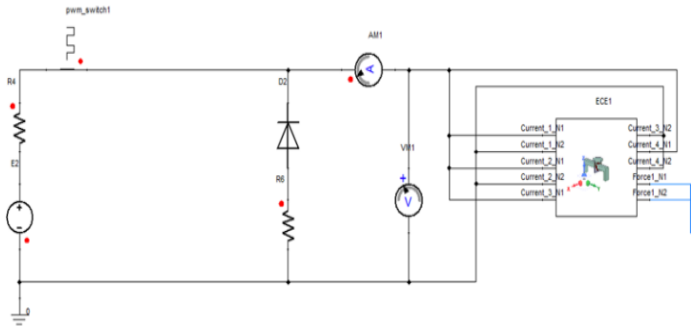

Fig. 7. Electrical side of the QES power circuit

When the sensible technique is used, the relationship between the translational mass block, which represents the force displacement, and the translational limit stop block, which means the force displacement, can be seen in Fig. 10.

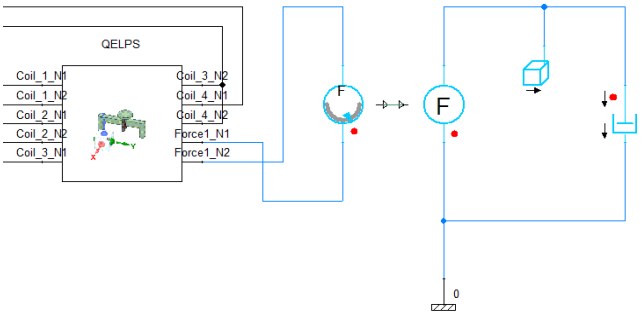

Fig. 8. Mechanical side of the QES power circuit

The armature sliding bar's damping coefficient was 100,000 Ns/m at a mass of 1000 grams. It has restrictions of 0.05 meters at the top and 0.01 meters at the bottom. To study the system's operational behavior, translational mass, and friction are connected by force output. In the translational friction model of the QES, the spring rate is considered 8 × 105 N/m and 10 × 105 Ns/m as the damping coefficients. The projectile Lorentz force generated in the coils was measured using a force meter, and the QES translational mechanical circuit is depicted in Fig. 8.

The ANSYS Simplorer circuit displayed the corresponding mass and damping. After execution, Fig. 9, 10, and 11 show the square-shaped yoke's force, current, and velocity. Fig. 9 shows the force plots of the QES for the two cycles. The force graphs of the QES for the two cycles are shown in Figure 9. When the PWM switch is turned on, the Lorentz force increases to 27.6 newtons after a one-millisecond delay, depending on the needed pulse width for operation.

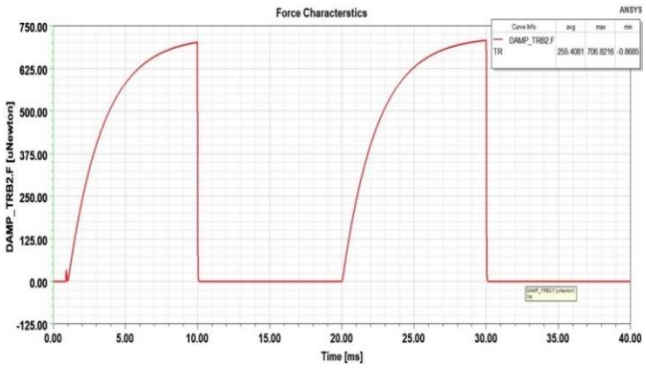

Fig. 9. QES Force Profile

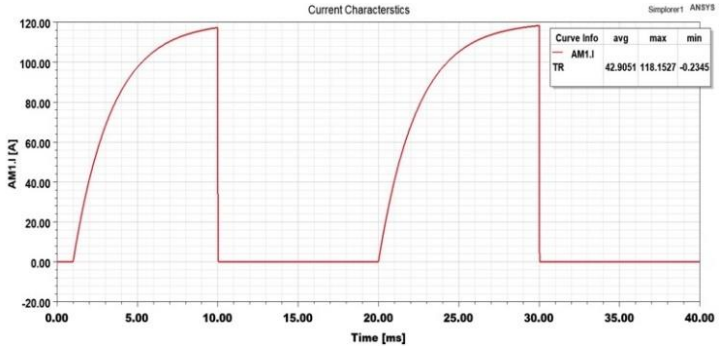

Fig. 10. QES Current Profile

The force returned to its baseline after the PWM switch was switched off. During this cycle of turning the PWM switch on and off, the QES may continue to operate smoothly along its linear path. This study represents a fundamental investigation of incorporating QES in linear motion tracking systems.

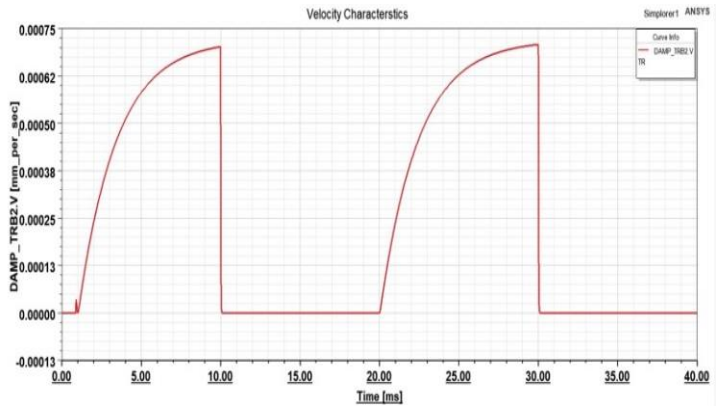

Fig. 11. QES Velocity Profile

Fig. 11 shows a plot of time and velocity in milliseconds. Upon activating the PWM switch, the velocity increases to 0.00074 mm/s. The second half of the cycle saw no variation in speed while the PWM switch was in its on state. At this point, there was a rise in velocity to 0.0014 mm/s when the switch was ON, and the velocity remained constant.

VI. Conclusion

In this article, the design and modeling of the quadrupole electromagnetic system (QES), which is a non-contact linear moving system that precisely reaches the desired position, have been comprehensively presented. In contrast to the four-track system, the QES design prioritizes reducing rail-armature contact sliding. ANSYS software is used for 3D modeling and magnetic properties analysis, and ANSYS Simplorer is used to simulate the power circuit during the design phase. The QES generates a consistent magnetic field inside the metal yoke. Position tracking requires a

strong, consistent magnetic field. The current density is highest in the yoke because of electromagnetic coils. Controlling the current density is essential to prevent the coils from overheating and breaking down the system.

According to the results, a force of 4kN was attained by particle swarm optimization (PSO). The paper includes design parameter optimization, electromagnetic and current characteristic modeling, and finite element analysis. The PSO method was executed ten times to determine the optimal design. The PSO runs yielded inductance values between 0.0164 mH and 0.0172 mH. This implies that the PSO algorithm yielded reliable outcomes. The PSO algorithm determines the optimal design of the QES, with optimal dimensions yielding a maximum force of 132 N. ANSYS Simplorer is used to simulate the power circuit and is developed using an ANSYS twin builder. The system performance can be analyzed by connecting the friction and friction and translational mass to the output of Lorentz force. The force profile in the QES is represented for two cycles, in which the maximum increase in Lorentz force is observed as 706 newtons with a one-millisecond initial delay. The PWM switch regulates the force profile, with an initial delay affecting the response.

VII. Acknowledgments

I wish to gratefully acknowledge my research supervisor, Dr K Sri Chandan, Assistant Professor at EECE, GITAM School of Technology. GITAM is deemed to be the University, Visakhapatnam, that provided insight and expertise that greatly assisted in articulating this research article.

Conflict of Interest

The authors declare that there are no conflicts of interest to disclose about the publishing of our research work in this article.

References

I. Cassat A., et al., : ‘Direct linear drives: Market and performance status’. *Proceedings of the 4th International Symposium on Linear Drives for Industry Applications. UK: Birmingham*, 2003.Boldea I, Naser SA. Linear motion electromagnetic systems. (First). Wiley-Interscience Hardcover, Fair, United Kingdom 1985.

II. Cupertino Francesco, et al., : ‘Sliding-mode control with double boundary layer for robust compensation of payload mass and friction in linear motors’. *IEEE Transactions on Industry Applications*. Vol. 45(5), pp. 1688-1696, 2009. 10.1109/TIA.2009.2027521

III. Dong Liang, Shuqi Sun, and Haiyang Wu., : ‘Study of capacitor parameters on the optimal trigger position of multipole field reconnection electromagnetic launcher’. *IEEE Transactions on Plasma Science*. Vol. 49(7), pp. 2153-2160, 2021. 10.1109/TPS.2021.3084632

IV. Engel Thomas G., and Michael J. Veracka. : 'The voltage–current scaling relationship and impedance of DC electromagnetic launchers'. *IEEE Transactions on Plasma Science*. Vol. 43(5), pp. 1271-1276. 2015. 10.1109/TPS.2015.2418053

V. Ferkova Z. et al., : 'Electromagnetic design of ironless permanent magnet synchronous linear motor'. *2008 International Symposium on Power Electronics, Electrical Drives, Automation and Motion. IEEE*, 2008. 10.1109/SPEEDHAM.2008.4581085

VI. Gordon Seamus, and Michael T. Hillery. 'Development of a high-speed CNC cutting machine using linear motors'. *Journal of Materials Processing Technology* Vol. 166(3), pp. 321-329, 2005. 10.1016/j.jmatprotec.2003.08.009

VII. Gutierrez Hector et al., : 'Non-contact DC electromagnetic propulsion by multipole transversal field: Numerical and experimental validation'. *IEEE Transactions on Magnetics*. Vol. 52(8), pp. 1-10, 2016. 10.1109/TMAG.2016.2553644

VIII. Kim Seog-Whan, Hyun-Kyo Jung, and Song-Yop Hahn. 'Optimal design of multistage coilgun'. *IEEE transactions on magnetics*. Vol. 32(2), pp. 505-508, 1996. 10.1109/20.486539.

IX. Kleinkes Michael, Werner Neddermeyer, and Michael Schnell. 'Improved method for highly accurate integration of track motions'. *ICINCO-RA.* 2006. 10.5220/0001203504690473

X. Kondamudi Sri Chandan et al., : 'A novel type coil-multipole field hybrid electromagnetic launching system'. *Results in Physics*. Vol. 15, 102786 2019. 10.1016/j.rinp.2019.102786.

XI. Kondamudi Srichandan, and Mallikarjuna Rao Pasumarthi. : 'Computations of magnetic forces in multipole field electromagnetic launcher'. *International Journal of Mathematical, Engineering and Management Sciences*. Vol. 4(3) pp. 761, 2019. 10.33889/IJMEMS.2019.4.3-059.

XII. Laithwaite Eric R. and Syed A. Nasar. : 'Linear-motion electrical machines'. *Proceedings of the IEEE*. Vol. 58(4) pp. 531-542, 1970. 10.1109/PROC.1970.7692.

XIII. Lesquesne B., : 'Permanent magnet linear motors for short strokes.' *Conference Record of the 1992 IEEE Industry Applications Society Annual Meeting. IEEE*. 1992. https://doi.org/10.1109/IAS.1992.244449.

XIV. Luo Wenbo et al., : 'Connection pattern research and experimental realization of single stage multipole field electromagnetic launcher'. *IEEE Transactions on Plasma Science*. Vol. 41(11), pp. 3173-3179, 2013. 10.1109/TPS.2013.2281240.

XV. Manohar Kintali, and Kondamudi Srichandan. : 'Analysis of Quadrupole Magnetic Field Reluctance-Based Launcher With Different Coil Switching Patterns'. *IEEE Transactions on Plasma Science*. 2023) 10.1109/TPS.2023.3266515.

XVI. Manohar Kintali, and Kondamudi Srichandan. : 'Design optimization of quad-pole electromagnetic ejection device using particle swarm optimization'. *IEEE International Conference on Intelligent Systems, Smart and Green Technologies (ICISSGT). IEEE*. 2021. 10.1109/ICISSGT52025.2021.00022.

XVII. Meinke R. B., C. L. Goodzeit, and M. J. Ball. : 'Modulated double-helix quadrupole magnets'. *IEEE transactions on applied superconductivity*. Vol. 13(2), pp. 1369-1372, 2003. 10.1109/TASC.2003.812674.

XVIII. Musolino Antonino, Rocco Rizzo, and Ernesto Tripodi. : 'Travelling wave multipole field electromagnetic launcher: An SOVP analytical model'. *IEEE Transactions on Plasma Science*. Vol. 41(5), pp. 1201-1208, 2013. https://doi.org/10.1109/TPS.2013.2246839.

XIX. Prasad Gajja, and Kondamudi Srichandan. : 'Performance Evaluation on Two Wing Ring Type Armature with Inductive Type Electromagnetic Launching System'. *IEEE 10th Power India International Conference* (PIICON). IEEE, 2022. 10.1109/PIICON56320.2022.10045133.

XX. Shokair Isaac R., : 'Projectile transverse motion and stability in electromagnetic induction launchers'. *IEEE transactions on magnetics*. Vol. 31(1), pp. 504-509, 1995. 10.1109/20.364641.

XXI. Thotakura Sandhya, Kondamudi Srichandan, and P. Mallikarjuna Rao. : 'A novel configuration of multi-stage outrunner electromagnetic launching for aircraft catapult system'. *Advances in Decision Sciences, Image Processing, Security and Computer Vision: International Conference on Emerging Trends in Engineering (ICETE)*. Vol. 2. Springer International Publishing, 2020. 10.1007/978-3-030-24318-0_44.

XXII. Xue Xinpeng, et al., : 'A new electromagnetic launcher by sextupole rails: Electromagnetic propulsion and shielding numerical validation'. *IEEE Transactions on Plasma Science*. Vol. 45(9), pp. 2541-2545, 2017. 10.1109/TPS.2017.2728688.

XXIII. Yan Zhongming, et al., : 'Study of single-stage double-armature multipole field electromagnetic launcher'. *IEEE Transactions on Plasma Science*. Vol. 45(8), pp. 2381-2386, 2017. 10.1109/TPS.2017.2716421.

XXIV. Yang Zhiyong et al., : 'An electromagnetic rail launcher by quadrupole magnetic field for heavy intelligent projectiles'. *IEEE Transactions on Plasma Science*. Vol. 45(7), pp. 1095-1100, 2017. 10.1109/TPS.2016.2646377.

XXV. Yingwei Zhu et al., : 'Analysis and evaluation of three-stage twisty octapole field electromagnetic launcher'. *IEEE Transactions on Plasma Science*. Vol. 40(5), pp. 1399-1406, 2012. 10.1109/TPS.2012.2188530.

XXVI. Zabar Z. et al. : 'Improved method for highly accurate integration of track motions'. *IEEE transactions on magnetics*. Vol. 25(1), pp. 627-631, 1989. 10.1109/20.22613.

XXVII. Zhu Yingwei et al., : 'Multipole field electromagnetic launcher'. *IEEE transactions on magnetics*. : Vol. 46(7), pp. 2622-2627, 2010. 10.1109/TMAG.2010.2044416.